Photon scattering in the giant dipole resonance region of ^{16}O

S. F. LeBrun, A. M. Nathan, and S. D. Hoblit

Nuclear Physics Laboratory and Department of Physics, University of Illinois at Urbana-Champaign, Champaign, Illinois 61820

Differential cross sections for elastic scattering of tagged, monochromatic photons have been measured on a water target for incident photon energies between 21.7 and 27.5 MeV and at scattering angles of 135° and 45°. These data are interpreted in terms of the total photoabsorption cross section in the region of the giant dipole resonance. We find that the data are reasonably consistent with previous direct measurements of the total photoabsorption cross section and inconsistent with more recent determinations of the total cross section by summing the various partial cross sections.

I. INTRODUCTION

The giant dipole resonance (GDR) of ^{16}O has been the subject of considerable investigations, both theoretical and experimental, for the last 30 years. It is therefore rather surprising that the total photoabsorption cross section in the energy region spanning the GDR is still controversial. Of particular interest is the parameter κ, where $1+\kappa$ is the integral of the photoabsorption cross section σ_γ up to the meson threshold (~ 140 MeV) in units of the classical Thomas-Reiche-Kuhn (TRK) dipole sum rule ($60NZ/A$ MeV mb). The deviation of κ from zero is usually interpreted as an effect due to meson exchange currents, and it is particularly interesting to know how it depends on A. Photoneutron data from Saclay[1] show that κ is equal to the nearly constant value of ~ 0.76 for several medium and heavy nuclei between ^{90}Zr and ^{238}U. Photon scattering data from Illinois[2] suggest that this same constant value might extend at least as far down as ^{40}Ca. On the other hand, total photoabsorption data from Mainz[3] on light nuclei ($A \leq 40$) show considerably more variations in κ, which ranges from 0.42 for ^{9}Be to 1.07 for ^{40}Ca. The question of the dependency of κ on A has led to several attempts to reevaluate the total photoabsorption cross section, especially for light nuclei. The most extensive effort thus far has been for ^{16}O, which we now summarize.

Three different techniques have been used to determine σ_γ for ^{16}O: direct measurements of the total photon absorption, corrected for the (dominant) atomic photon absorption;[3-5] summation of partial cross sections in the various decay channels;[6,7] and indirect measurements via elastic photon scattering.[8] Various results from these studies for the integrated photoabsorption cross section are summarized in Table I. For ease of discussion, we define $\sigma_0(E_0)$ to be the integral of the photoabsorption cross section up to the energy E_0, in units of either MeV mb or the TRK sum rule, which is 240 MeV mb for ^{16}O. By far the most extensive direct measurements come from Mainz,[3] where the data extend from about 10 MeV up to well over the meson threshold. These measurements find 0.90 TRK up to 30 MeV and 1.95 TRK up to 140 MeV. More recent but less extensive measurements[4,5] find somewhat less strength (0.76±0.07 TRK up to 30 MeV). Two recent evaluations of the partial cross sections have been

performed,[6,7] and they find σ_0 (30 MeV)=0.65 TRK. In addition, Berman et al.[6] have extended the evaluation up to 140 MeV, and find σ_0 (140 MeV)=1.40 TRK. Finally, photon scattering measurements between 25 and 40 MeV from the National Bureau of Standards are found to be consistent with the photoabsorption[3] only if the Mainz total (nuclear plus atomic) cross sections are scaled down by 0.997. This would imply σ_0 (30 MeV)=0.78 TRK. Thus, referring to the summary in Table I, there are values for σ_0 (30 MeV) ranging from 0.65 to 0.90 TRK and for σ_0(140 MeV) ranging from 1.40 to 1.95 TRK. Recall that the corresponding value of σ_0 (140 MeV) for medium and heavy nuclei is 1.76. Needless to say, the implication of the discrepancies in ^{16}O is profound for any model that attempts to predict the A dependence of κ.

The present work attempts to address this problem indirectly through elastic photon scattering measurements over an energy range spanning the GDR region. Specifically we have measured the elastic scattering cross sections at angles of 135° and 45° for 32 different energies between 21.7 and 27.5 MeV. We have used these data to "extract" the photoabsorption cross section over that same energy range, using a formalism that has been successfully applied and described elsewhere.[2,8,9] We find that these scattering data strongly support the Mainz cross sections in the 21.5—30 MeV range and are inconsistent with the smaller cross section deduced by summing the partial cross sections.

The outline of the remainder of this paper is as follows. In Sec. II we discuss experimental aspects of this work. The interpretation of the elastic scattering data in terms of σ_γ is presented in Sec. III. We summarize our conclusions in Sec. IV.

II. EXPERIMENTAL PROCEDURE AND DATA REDUCTION

Elastic scattering cross sections on a water target were measured using incident photon beams from the Illinois tagged photon facility and using a large-crystal NaI spectrometer to detect the scattered photons. Both the experimental technique and the method used to extract absolute

TABLE I. Measured values of $\sigma_0(E_0) = \int_0^{E_0} \sigma_\gamma(E)dE$. The numbers in parentheses indicate $\sigma_0(E_0)$ in units of the TRK sum (240 MeV mb).

Technique[a]	$\sigma_0(E)$ (MeV mb) $E_0 = 30$ MeV	$E_0 = 140$ MeV
TPA[b]	216.2 (0.90)	469.0 (1.95)
TPA[c]	182±17 (0.76)	
SOP[d]	155±18 (0.65)	336±36 (1.40)
SOP[e]	154±9 (0.65)	
PS[f]	186 (0.78)	
PS[g]	210±14 (0.88)	

[a]TPA means total photon absorption; SOP means sum of partial cross section; PS means photon scattering.

[b]Reference 3.

[c]References 4 and 5.

[d]Reference 6.

[e]Reference 7. The authors of Ref. 7 quote σ_0 (29 MeV) = 147±9 MeV mb. From the original references, we estimate an additional contribution of 7 MeV mb between 29 and 30 MeV. On the other hand, the authors of Ref. 6 quote a preliminary report from the authors of Ref. 7 in which σ_0 (30 MeV) = 169±18 MeV mb.

[f]Reference 8.

[g]Present results; these results were derived by summing the Mainz cross section (Ref. 3) up to 21.5 MeV and the best fit results for the scattering data from 21.5 to 30 MeV.

cross sections from the data have been described in previous publications,[2,9] and we only focus on the highlights here. Briefly, a few nA beam of 40.65 MeV electrons are focused onto a 34.3 mg/cm^2 Al foil, resulting in the emission of bremsstrahlung radiation, which interacts with the water target 2 m downstream of the radiator foil. Post-bremsstrahlung electrons are momentum analyzed in a magnetic spectrometer and detected in an array of 32 plastic scintillators in coincidence with the associated photon, which scattered from the water target into the NaI detector. Thus the photons are "tagged." The tagging range in the present experiment extended from 21.68 to 27.56 MeV in 32 contiguous bins. The scattering target was a 7.5-cm thick cell of water contained in a lucite box. Thin Mylar foils (each 20 μm thick) served as entrance and exit windows, and although no data were taken with an empty cell, it is conservatively estimated that less than 0.5% of the scattered photons originated from the windows.

The elastic scattering cross section, $d\sigma/d\Omega$, is given by

$$\frac{d\sigma}{d\Omega} = \frac{1}{k\Omega}\left[\frac{R_S}{R_B}\right], \tag{1}$$

where k is the number of target nuclei per unit area and Ω is the solid angle subtended by the detector. These latter parameters are calculated for an extended target using a Monte Carlo simulation which includes the effects of the finite size of the photon beam and the attenuation of photons in the target. In Eq. (1), R_S is the number of detected scattered photons per tagging electron, and R_B is the number of incident tagged photons in the beam per tag-

ging electron. The latter quantity is measured in a separate calibration experiment with the NaI placed directly into the photon beam.

Spectra of both total coincidences and chance coincidences are collected, and the net coincidence spectrum is obtained by subtracting the appropriately scaled accidental spectrum from the total coincidence spectrum. A typical spectrum at each angle is shown in Fig. 1, in which the elastic-scattering peak is clearly visible near channel 188. Also apparent in the 135° spectrum is a peak near channel 118 resulting from the decay of the 15.11-MeV level in ^{12}C, which is produced in the ^{16}O(γ,α) reaction.

The net yield of elastically scattered photons was extracted from the spectra either by summing the counts over the region of the elastic scattering peak or by scaling a parametrized response function to best fit the data. The response function was obtained in the calibration experiment with the detector placed directly into the tagged photon beam. These two techniques produced results that agreed to within a few percent. The resulting elastic scattering cross sections are listed in Table II. The uncertainties include statistical errors only. The systematic uncertainty in the absolute cross section scale is estimated to be ±7%. The results are displayed graphically in Fig. 2; also included are the earlier results of Dodge et al.,[8] which are in excellent agreement with the present cross
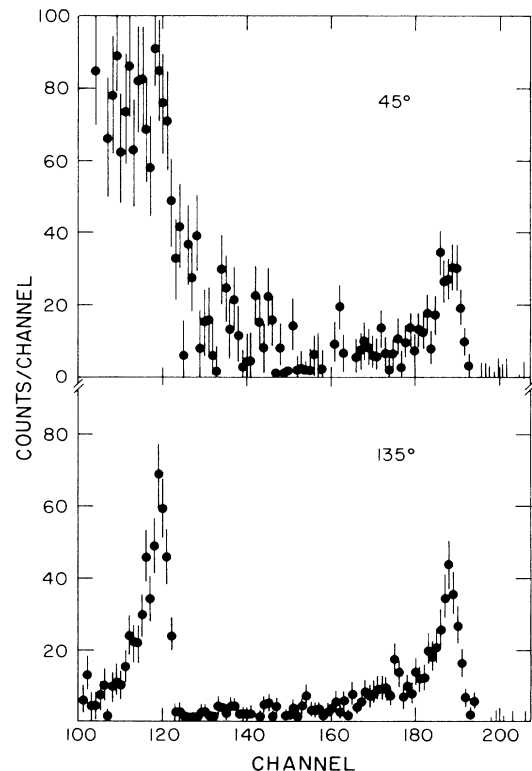
FIG. 1. Spectrum of photons scattered from a water target in a 24.55 MeV tagged photon beam. The energy scale is 0.13 MeV/channel. The peak near channel 188 corresponds to elastic scattering, while the one near channel 118 corresponds to the decay of the 15.11 MeV level in ^{12}C, which is produced via the photoalpha reaction. The steep background below channel 130 in the 45° spectrum is atomic in origin.

TABLE II. Elastic scattering cross section from ^{16}O. The numbers in parentheses indicate the statistical error on the cross section.

E (MeV)	$d\sigma/d\Omega$ (μb/sr)	
	$\theta = 135°$	$\theta = 45°$
21.68	3.60 (27)	4.53 (56)
21.84	5.25 (32)	4.85 (59)
22.00	6.84 (37)	7.41 (65)
22.15	7.89 (39)	9.65 (67)
22.30	9.20 (42)	9.32 (67)
22.46	7.18 (36)	7.63 (59)
22.62	4.23 (31)	3.96 (56)
22.77	3.12 (25)	4.43 (51)
22.93	6.21 (34)	7.47 (58)
23.11	5.92 (32)	6.33 (53)
23.30	4.31 (35)	4.86 (58)
23.49	3.35 (27)	4.34 (51)
23.67	3.13 (27)	3.88 (48)
23.84	2.85 (25)	3.32 (45)
24.01	4.14 (28)	4.80 (47)
24.18	6.62 (35)	7.08 (53)
24.36	6.52 (36)	6.36 (52)
24.55	4.79 (29)	5.40 (45)
24.76	4.89 (31)	5.22 (48)
24.96	4.81 (30)	5.21 (45)
25.15	5.05 (30)	6.12 (45)
25.36	4.91 (30)	5.42 (45)
25.58	5.33 (33)	4.97 (45)
25.78	4.63 (28)	5.83 (45)
25.98	4.74 (30)	4.62 (41)
26.19	3.51 (27)	4.85 (43)
26.42	3.78 (26)	3.37 (36)
26.64	3.68 (27)	4.23 (41)
26.86	4.05 (27)	3.51 (37)
27.14	3.49 (27)	4.05 (39)
27.39	3.48 (25)	3.28 (35)
27.56	2.91 (23)	3.24 (34)

FIG. 2. Elastic scattering cross sections at (a) 135° and (b) 45° from ^{16}O. The error bars are statistical only. The open points are from Dodge et al. (Ref. 8). The solid curves are the predicted cross sections based on a multi-Lorentzian fit to the data, as described in the text. The dashed curves are the cross sections predicted directly from the photoabsorption cross sections of Ahrens et al. (Ref. 3).

sections. In comparing the present data with predictions based on various representations of the photoabsorption cross section (see Sec. III), we found it necessary to shift the energy of the present data downward by 0.17 MeV. Accordingly the numbers in Table II and Fig. 2 have already been shifted by that amount which is, however, within the estimated accuracy of the Hall probe used to measure the magnetic field of the tagging spectrometer.

III. ANALYSIS OF THE ELASTIC SCATTERING CROSS SECTIONS

A. General considerations

In this section, we discuss the formalism which allows us to infer the photoabsorption cross section $\sigma_\gamma(E)$ from the elastic scattering cross section $d\sigma/d\Omega(E,\theta)$. The essence of our technique[2,8,9] is the unique relationship between the complex forward scattering amplitude $R(E,\theta=0°)$ and $\sigma_\gamma(E)$ through the optical theorem

$$\mathrm{Im}[R(E,\theta=0°)] = \frac{E}{4\pi\hbar c}\sigma_\gamma(E) \qquad (2)$$

and a dispersion relation

$$\mathrm{Re}[R(E,\theta=0°)] = \frac{E^2}{2\pi^2\hbar c} P \int_0^\infty \frac{\sigma_\gamma(E')dE'}{E'^2 - E^2} + D , \qquad (3)$$

where P denotes the principal value of the integral and D is the Thomson amplitude. These relations imply that a knowledge of $\sigma_\gamma(E)$ at all energies uniquely determines the forward amplitude and therefore the forward cross section. In general one cannot easily reverse the process. That is, a measurement of $d\sigma/d\Omega(E,\theta)$ does not uniquely determine $\sigma_\gamma(E)$ unless $d\sigma/d\Omega(E,\theta)$ is known over the full range of energies for which $\sigma_\gamma(E)$ makes important contributions to the dispersion integral. However, at certain energies E_1 where the scattering amplitude is known to be dominated by the imaginary part, the optical theorem uniquely relates $\sigma_\gamma(E_1)$ to the scattering cross section. As we shall see shortly, in the energy range between 21 and 25 MeV in ^{16}O, the scattering amplitude is predominantly imaginary, so that it should be possible to place tight constraints on $\sigma_\gamma(E)$ in that range from the scattering measurements.

Of course, one cannot measure the forward scattering cross sections. However, the angular distribution of the elastically scattered photons is well known in the GDR region, so that $d\sigma/d\Omega(E,\theta=0°)$ can be inferred from measurements at other angles. Specifically, the scattering amplitude can be determined in a model-independent way

from the forward amplitude, and therefore from $\sigma_\gamma(E)$, provided the long-wavelength (LWL) limit is valid, the multipole composition of $\sigma_\gamma(E)$ is known, and D is corrected for a variety of effects. These effects include the finite size of the nucleus, meson exchange currents, and the structure of the nucleon. For scattering from light nuclei (such as ^{16}O) at energies not too large (e.g., < 30 MeV), the LWL approximation is valid. Furthermore, the modifications to the Thomson amplitude are either easily calculable from the known charge distribution (in the case of the finite-size correction), negligible (in the case of the structure of the nucleon), or completely specified by low-energy theorems (in the case of the mesonic effects). Finally, for scattering in the GDR region the $E1$ multipole dominates the other multipoles. Therefore the principal effect of the major competing multipole $E2$ would be to introduce a fore-aft asymmetry into the scattering cross section section due to the interference of the $E2$ with the dominant $E1$. Since the present data were taken at symmetric forward and backward angles, the interference cancels in the angle-averaged scattering data, which are therefore very insensitive to small amounts of $E2$ strength. Actually the scattering data themselves seem to rule out large amounts of $E2$ strength since the fore-aft ratios are essentially consistent with purely $E1$. Therefore, it is safe to analyze the data as though $\sigma_\gamma(E)$ were all $E1$.

To summarize, Eqs. (2) and (3) allow one to calculate the scattering cross section that is predicted by a particular choice of $\sigma_\gamma(E)$, where $\sigma_\gamma(E)$ is assumed to be purely $E1$ and the appropriate (model-independent) corrections are made to the Thomson amplitude. This allows one to test the overall consistency between the measured scattering cross sections and the choice of $\sigma_\gamma(E)$. For example, if there is an experimental determination of $\sigma_\gamma(E)$, one can examine the overall consistency with the scattering data. Alternatively, one can parametrize $\sigma_\gamma(E)$ (e.g., as a sum of Lorentzian lines) and adjust the parameters to best fit the available data (scattering and/or photoabsorption). We utilize both techniques in the analysis to follow.

B. Determination of $\sigma_\gamma(E)$ in the GDR region

We start by using the preceding formalism to calculate the scattering cross sections predicted by the $\sigma_\gamma(E)$ of Ahrens et al.[3] (the Mainz data). These data[10] are different from the original published data in that they have been corrected slightly for a change in energy scale (which tends to reduce the lower-energy cross sections). Additionally, they have been corrected approximately for the in-scattering of photons. This correction makes the cross sections larger, especially at low energies. These data, which extend from 12 to 140 MeV, are shown as the closed points in Fig. 3(a) over the 20—30 MeV range. For these calculations, the principal value integral of Eq. (3) is performed numerically. The resulting prediction for the 135° and 45° scattering cross sections is shown as the dashed line in Fig. 2, and the corresponding forward scattering amplitude is shown in Fig. 3(b). The general trend of the data is accounted for by the calculations, especially above 25 MeV where the cross section varies
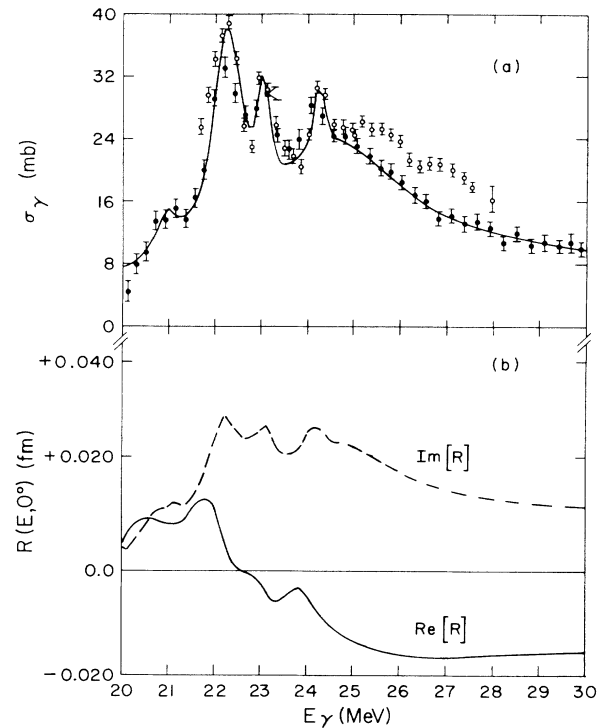
FIG. 3. (a) Photoabsorption cross section in ^{16}O. The closed points are the data of Ahrens et al. (Ref. 3), and the open points are upper limits on σ_γ determined directly from the elastic scattering cross section via the optical theorem. The curve is the multi-Lorentzian fit to the scattering data and corresponds to the cross section used to predict the solid curve in Fig. 2. (b) The real and imaginary parts of the forward scattering amplitude calculated from the photoabsorption cross section of Ahrens et al.

more smoothly with energy. However, below 25 MeV the data show somewhat sharper structure than the calculation, that is, both larger maxima and deeper minima. This is possibly due to the energy averaging in the Mainz data set. In fact, both the (γ,p_0) (Ref. 11) and the (γ,n_0) (Ref. 12) cross sections show sharper structure than the Mainz cross section in the 21—25 MeV region.

In order to better emphasize the overall consistency between the Mainz data and the scattering data, we plot as open points in Fig. 3(a) upper bounds on $\sigma_\gamma(E)$ implied by the average of the 135° and 45° scattering data. These points are derived by assuming the scattering amplitude is purely imaginary and applying the optical theorem [Eq. (2)]; the upper bounds become equalities whenever the real amplitude vanishes. Before comparing these points with the Mainz data, we first remark that Fig. 3(b) shows that there is a wide range of energies, 22.2—25 MeV, over which the imaginary amplitude dominates. This energy range is only weakly independent on the specifics of the Mainz cross sections, which were used to compute the dispersion integral. In fact, the energy at which the real amplitude changes sign is largely determined by the global shape of the photoabsorption cross section, which is not seriously in question in this case. For ^{16}O, this range of

energies is particularly large because of the superposition of finer structure upon the overall shape of the GDR, thereby causing the real amplitude to oscillate about a value close to zero. We have verified by direct calculation that other reasonable representations[7] of $\sigma_\gamma(E)$ predict essentially the same range of energies for the real amplitude to be negligible. Thus, we expect the open points in Fig. 3(a) to be quite good estimates of $\sigma_\gamma(E)$ over the 22.2—25 MeV energy range. Figure 3(a) shows that in that range, there is reasonable agreement between the open points and the (Mainz) closed points. In fact, the open points seem to oscillate about the Mainz data, suggesting that the structure in $\sigma_\gamma(E)$ in this region is somewhat narrower than implied by the Mainz data. Nevertheless, the *integral* agreement between 22.2 and 25 MeV is quite good. Above 25 MeV, where the real amplitude is no longer negligible, the upper limits are indeed well above the Mainz points, as expected.

We next ask whether we can improve on the Mainz cross sections by finding a photoabsorption cross section even more consistent with the scattering data. We first observe that it is possible to parametrize the Mainz data as a sum of eight Lorentzian lines (all centered below 30 MeV) plus a small quasideuteron (QD) tail that drops smoothly to zero between 30 MeV and 280 MeV. We therefore attempt to adjust the centroid, peak absorption, and width of each Lorentzian as well as the amplitude (but not the shape) of the QD tail in order to best fit the scattering data. In so doing, it is necessary to provide some means of constraining $\sigma_\gamma(E)$ outside the energy range of the scattering data. We use the Mainz data themselves to provide such a constraint. That is, we fit the parametrized cross sections simultaneously to the scattering data and the Mainz data, excluding the Mainz data between 21.5 and 30 MeV. Based on the remarks above about the dominance of the imaginary amplitude, we expect that the resulting best-fit $\sigma_\gamma(E)$ in the 21.5—30 MeV energy range will be determined essentially by the scattering data alone, and in particular that it is not very sensitive to the use of the Mainz data to constrain $\sigma_\gamma(E)$ outside that range. In fact, we will explicitly show that this is true below.

The resulting $\sigma_\gamma(E)$ is compared to the Mainz data in the curve of Fig. 3(a), and the predicted scattering cross sections are shown as the solid curves in Fig. 2. The Lorentzian and QD parametrizations are listed in Tables

TABLE III. Best-fit Lorentzian parametrization of $\sigma_\gamma(E)$ corresponding to the curve in Fig. 3.

E_0 (MeV)	σ_0 (mb)	Γ_0 (MeV)
13.12	5.96	0.45
17.27	8.69	0.15
20.94	5.51	0.53
22.24	27.48	0.70
23.02	16.27	0.23
24.23	11.21	0.17
24.63	15.23	3.45
28.22	6.97	19.52

TABLE IV. Quasideuteron tail used in the best-fit $\sigma_\gamma(E)$ corresponding to the curve in Fig. 3. The cross section is a piecewise linear curve connecting the tabulated points.

E (MeV)	σ (mb)
12	0
20	1.62
40	1.41
80	1.06
140	0.86
280	0

III and IV, respectively. It is clear from these figures that there is excellent consistency of this $\sigma_\gamma(E)$ with both the scattering data and the Mainz data. Indeed, it appears that the only significant difference with the Mainz data is that the parametrized $\sigma_\gamma(E)$ seems to have sharper structure between 22 and 25 MeV; as noted above, this may be due simply to the finite energy resolution of the Mainz data. One measure of the overall consistency is in the integrated cross section between 21.5 and 30 MeV: the Mainz data has 166 MeV mb whereas the fit has 164 MeV mb. The consistency between the elastic scattering cross sections and the Mainz data represents the principal result of this work.

We next investigate the sensitivity of our inferred σ_γ in the 21.5—30 MeV range (the range of interest) to σ_γ outside that range. Therefore we repeated the procedure described above with different choices for σ_γ outside the region of interest. We find, as expected, that our results are quite insensitive to reasonable variations in σ_γ. An extreme example is shown in Fig. 4. The solid curve is the same best-fit value of σ_γ as the curve in Fig. 3(a). The dashed curve is the best-fit σ_γ derived by assuming σ_γ outside the region of interest is the Mainz cross section
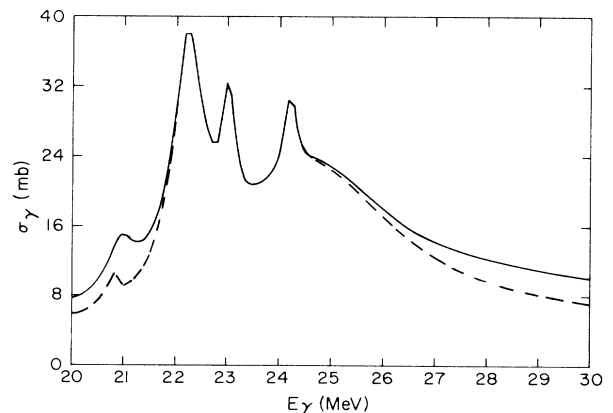
FIG. 4. Multi-Lorentzian representations of $\sigma_\gamma(E)$ based on various fits to the scattering data and the Mainz photoabsorption scaled by the factor $f = 1.0$ (solid line) and $f = 0.7$ (dashed line). As discussed in the text, these curves demonstrate the insensitivity of $\sigma_\gamma(E)$ derived from the scattering data to the photoabsorption cross section outside the 21.5—30 MeV range.

scaled by 0.7. The two curves nearly coincide between 21.5 and 25 MeV and slowly diverge from each other between 25 and 30 MeV. In fact the integrated sums between 21.5 and 30 MeV are not very different: 164 and 151 MeV mb for the solid and dashed curves, respectively. Thus we conclude that our results are not very sensitive to σ_γ outside the 21.5—30 MeV range.

Finally we investigate the sensitivity of our conclusion to the absolute scale of the scattering cross sections. We repeated the above procedures with the scattering data scaled up or down by 7%, the estimated overall accuracy of the data. We conclude that the integrated photoabsorption cross section between 21.5 and 30 MeV has a best-fit value of 163 ± 7 MeV mb (compared to 166 MeV mb for the Mainz data). Linking onto the Mainz data below 21.5 MeV results in an integrated sum up to 30 MeV of 210 ± 14 MeV mb. This value is compared to other determinations in Table I. In particular, the present result is not grossly inconsistent with either the total photon absorption measurements of Sherman, et al.[4,5] or the photon scattering measurements of Dodge, et al.,[8] but it is quite inconsistent with either of the recent attempts to sum the partial cross sections.[6,7]

It is interesting to speculate on the implications of our result for the parameter κ. If our value of σ_0 (30 MeV) is summed with the integral of the Mainz cross section between 30 and 140 MeV, this implies $\kappa=0.93$, as compared to the values of 0.95 and 0.40 from the Mainz data and

the sum of partial cross sections, respectively. On the other hand, if our result is added to the sum of partial cross sections above 30 MeV, this implies $\kappa=0.63$. This latter value is close to the value 0.76 for medium and heavy nuclei. Clearly this uncertainty in κ points to the need for new measurements of σ_γ in the 30—140 MeV range.

IV. SUMMARY

We have measured cross sections for the elastic scattering of photons on ^{16}O between 21.7 and 27.5 MeV. From these data we have extracted the photoabsorption cross section in the GDR region and have shown that it is in substantial agreement with the direct measurements from Mainz. We have further found that our data are inconsistent with recent attempts to determine the photoabsorption by summing the various partial cross sections.

ACKNOWLEDGMENTS

[1]A. Lepretre, H. Beil, R. Bergere, P. Carlos, J. Fagot, A. de Miniac, and A. Veyssière, Nucl. Phys. A 367, 327 (1981).

[2]D. H. Wright, P. T. Debevec, L. J. Morford, and A. M. Nathan, Phys. Rev. C 32, 1174 (1985).

[3]J. Ahrens, H. Borchert, K. H. Czock, H. B. Eppler, H. Gimm, H. Gundrum, M. Kroning, P. Riehn, G. Sita Ram, A. Zieger, and B. Ziegler, Nucl. Phys. A 251, 479 (1975).

[4]N. K. Sherman, W. F. Davidson, and A. Claude, J. Phys. G 9, 1519 (1983).

[5]N. K. Sherman, W. F. Davidson, S. Raman, W. Delbianco, and G. Kajrys, in Capture Gamma-Ray Spectroscopy and Related Topics, edited by S. Raman (AIP, New York, 1985), p. 221.

[6]B. L. Berman, R. Bergere, and P. Carlos, Phys. Rev. C 26, 304 (1982).

[7]E. G. Fuller, Phys. Rep. 127, 185 (1985).

[8]W. R. Dodge, E. Hayward, R. G. Leicht, M. McCord, and R. Starr, Phys. Rev. C 28, 8 (1983).

[9]A. M. Nathan, P. L. Cole, P. T. Debevec, S. D. Hoblit, S. F. LeBrun, and D. H. Wright, Phys. Rev. C 34, 480 (1986).

[10]J. Ahrens, private communication.

[11]W. J. O'Connell and S. S. Hanna, Phys. Rev. C 17, 892 (1978).

[12]J. W. Jury, J. S. Hewitt, and K. G. McNeill, Can. J. Phys. 48, 1635 (1970).